AGU PUBLICATIONS

Paleoceanography

RESEARCH ARTICLE
10.1002/2016PA002994

Key Points:
- Expansion of Glacial North Pacific Intermediate Water (GNPIW) to the tropical Pacific
- Glacial switch to additional influence of GNPIW at the Eastern Equatorial Pacific
- Enhanced GNPIW convection coincides with low-latitude nutrient and marine productivity changes

Supporting Information:
- Table S1
- Table S2

Correspondence to:
L. Max,
Lars.Max@awi.de

Citation:
Max, L., N. Rippert, L. Lembke-Jene, A. Mackensen, D. Nürnberg, and R. Tiedemann (2017), Evidence for enhanced convection of North Pacific Intermediate Water to the low-latitude Pacific under glacial conditions, *Paleoceanography*, *32*, 41–55, doi:10.1002/2016PA002994.

Received 27 JUN 2016
Accepted 21 DEC 2016
Accepted article online 26 DEC 2016
Published online 20 JAN 2017

Evidence for enhanced convection of North Pacific Intermediate Water to the low-latitude Pacific under glacial conditions

L. Max[1], N. Rippert[1], L. Lembke-Jene[1], A. Mackensen[1], D. Nürnberg[2], and R. Tiedemann[1]

[1]Alfred Wegener Institute, Helmholtz Centre for Polar and Marine Research, Bremerhaven, Germany, [2]GEOMAR Helmholtz Centre for Ocean Research Kiel, Kiel, Germany

Abstract We provide high-resolution foraminiferal stable carbon isotope ($\delta^{13}C$) records from the subarctic Pacific and Eastern Equatorial Pacific (EEP) to investigate circulation dynamics between the extratropical and tropical North Pacific during the past 60 kyr. We measured the $\delta^{13}C$ composition of the epibenthic foraminiferal species *Cibicides lobatulus* from a shallow sediment core recovered from the western Bering Sea (SO201-2-101KL; 58°52.52′N, 170°41.45′E; 630 m water depth) to reconstruct past ventilation changes close to the source region of Glacial North Pacific Intermediate Water (GNPIW). Information regarding glacial changes in the $\delta^{13}C$ of subthermocline water masses in the EEP is derived from the deep-dwelling planktonic foraminifera *Globorotaloides hexagonus* at ODP Site 1240 (00°01.31′N, 82°27.76′W; 2921 m water depth). Apparent similarities in the long-term evolution of $\delta^{13}C$ between GNPIW, intermediate waters in the eastern tropical North Pacific and subthermocline water masses in the EEP suggest the expansion of relatively ^{13}C-depleted, nutrient-enriched, and northern sourced intermediate waters to the equatorial Pacific under glacial conditions. Further, it appears that additional influence of GNPIW to the tropical Pacific is consistent with changes in nutrient distribution and biological productivity in surface waters of the glacial EEP. Our findings highlight potential links between North Pacific mid-depth circulation changes, nutrient cycling, and biological productivity in the equatorial Pacific under glacial boundary conditions.

1. Introduction

The high latitudes of the North Pacific and the Southern Ocean play an essential role in regulating the exchange of CO_2 between the ocean and the atmosphere [*Takahashi et al.*, 2002]. In both regions, vertical mixing brings nutrient- and CO_2-rich deep waters into the euphotic zone and facilitates the biological pump, which sequesters atmospheric CO_2 back into the deeper ocean interior [e.g., *Honda et al.*, 2002]. In the modern North Pacific, however, the further exposure of nutrient- and CO_2-rich subsurface waters to the surface ocean is largely hampered by a permanent halocline [*Haug et al.*, 1999]. In both regions, intermediate water masses are formed that recirculate excess nutrients from the high-latitude oceans toward the low-latitude regions of the Pacific Ocean (Figure 1). North Pacific Intermediate Water (NPIW) is formed in the subsurface of the Northwest Pacific via mixing of high-nutrient subsurface waters and intermediate water masses produced in coastal polynyas through brine rejection during wintertime sea ice production in the Okhotsk Sea [*Talley*, 1993; *Shcherbina et al.*, 2003]. Today, NPIW circulates within the upper ~ 300–800 m and is mainly restricted to the subtropical North Pacific regions between ~ 20°N and 40°N; however, a tongue of NPIW also spreads into the Celebes Sea in the western tropical Pacific [*Talley*, 1993; *Bostock et al.*, 2010]. In the Southern Ocean Antarctic Intermediate Water (AAIW) is produced at the surface ocean from upwelled nutrient- and CO_2-enriched Circumpolar Deep Water (CDW). AAIW further ventilates into the Subtropical Gyre and thereby transports heat, salt, and other chemical species, including dissolved CO_2, from the high latitudes of the Southern Ocean toward the equatorial Pacific. This, so-called "ocean tunneling" is one major process that provides nutrients to tropical Pacific thermocline waters today [e.g., *Bostock et al.*, 2010] (Figure 1).

An important difference between northern and southern sourced intermediate waters is that subsurface formation of NPIW largely prevents the biologically driven resetting of deep ocean nutrient ratios that happens at the surface ocean during formation of AAIW. It is for this reason that NPIW is characterized by higher silicic acid to nitrate supply ratios compared to southern sourced intermediate waters [*Sarmiento et al.*, 2004] (Figure 1). On the other hand, as carbon fixation is dominated by siliceous phytoplankton at the surface ocean near the formation region of modern AAIW, southern sourced intermediate waters are characterized by high

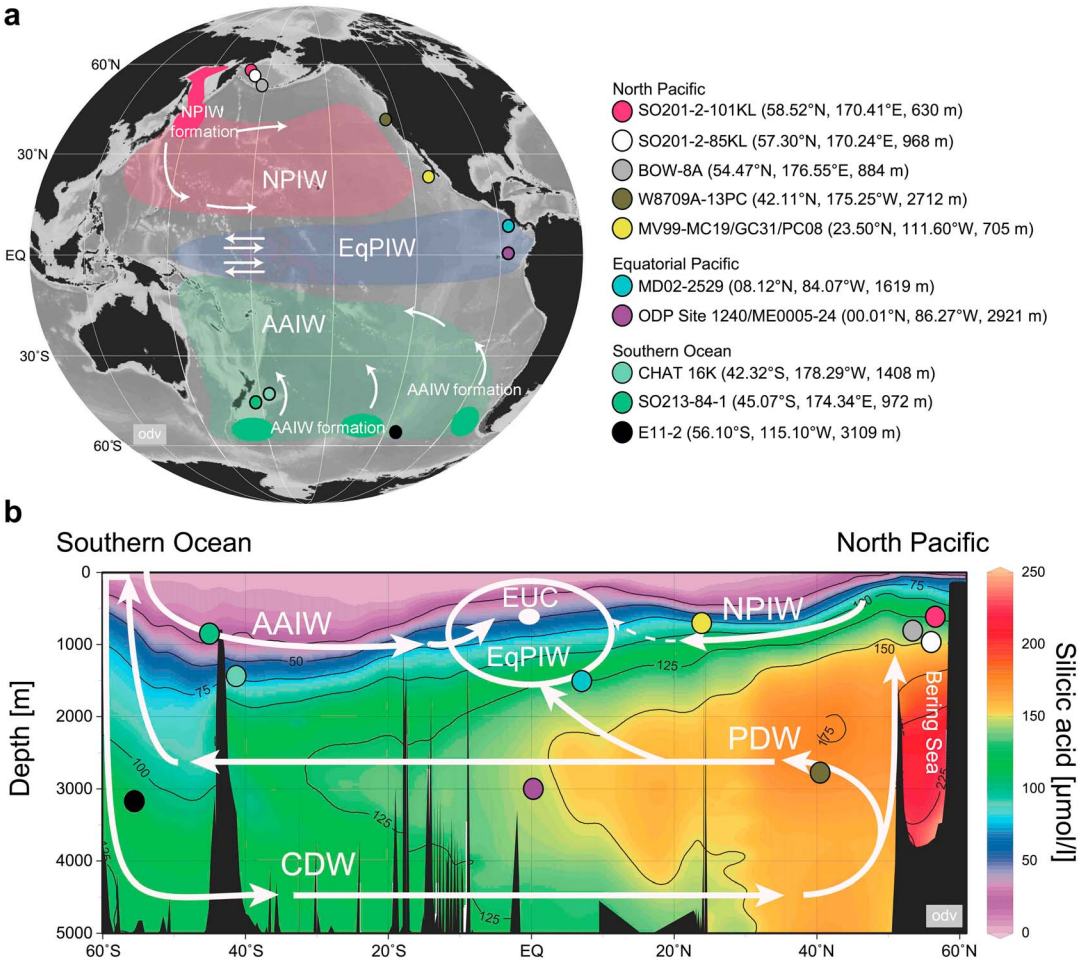

Figure 1. (a) Bathymetric chart of the Pacific Ocean with locations of proxy records in the North Pacific (SO201-2-101KL, this study; SO201-2-85KL [*Max et al.*, 2012]; BOW-8A [*Horikawa et al.*, 2010]; W8709A-13PC [*Lund and Mix*, 1998]; MV99-MC19/GC31/PC08 [*Basak et al.*, 2010]), the equatorial Pacific (MD02-2529 [*Leduc et al.*, 2010]; ODP Site 1240 [*Pichevin et al.*, 2009; this study]; ME0005-24 [*Kienast et al.*, 2007]), and the Southern Ocean (CHAT 16K [*Noble et al.*, 2013]; SO213-84-1 [*Ronge et al.*, 2015]; E11-2 [*Robinson et al.*, 2014]) considered in this study. White arrows denote major circulation pattern of intermediate water masses in the North Pacific and Southern Ocean. Magenta and green spots indicate formation regions of AAIW and NPIW, and shaded magenta and green areas mark modern lateral extent of intermediate waters in the Pacific Ocean. (b) Meridional section of present-day silicic acid concentrations from the North Pacific to the Southern Ocean [*Garcia et al.*, 2010] and major modern mid-depth to deep-water masses (white arrows): AAIW = Antarctic Intermediate Water; CDW = Circumpolar Deep Water; EUC = Equatorial Undercurrent; EqPIW = Equatorial Pacific Intermediate Water; NPIW = North Pacific Intermediate water; PDW = Pacific Deep Water (modified after *Bostock et al.* [2010]). This figure was generated with Ocean Data View [*Schlitzer*, 2015].

nitrate, but low silicic acid concentrations [*Sarmiento et al.*, 2004] (Figure 1). Under modern conditions, mainly southern sourced water masses (AAIW) are injected into the eastward directed Equatorial Undercurrent (EUC) and the Equatorial Pacific Intermediate Water (EqPIW) via the South Equatorial Current and the New Guinea Coastal Undercurrent [*Dugdale et al.*, 2002]. The dominant role of AAIW on equatorial intermediate waters was also verified by a geochemical tracer analyses that suggests that EqPIW are primarily a combination of AAIW and Pacific Deep Water (PDW) with only a very minor contribution of NPIW today [*Bostock et al.*, 2010] (Figure 1). As the intermediate water masses flow toward the east, they supply nutrients via diapycnal mixing to the overlying waters masses [*Rafter and Sigman*, 2016]. As a consequence of the high southern sourced contribution today, carbon fixation by siliceous phytoplankton is limited by low silicic acid and iron availability in the Eastern Equatorial Pacific (EEP), making this region a significant net source of CO_2 to the atmosphere [*Dugdale et al.*, 2002].

Information regarding past deep ocean circulation changes can be reconstructed from the stable carbon isotopic composition ($\delta^{13}C$) measured on benthic foraminiferal tests. During the past 30 years, this proxy has been successfully used to investigate glacial to interglacial changes in water mass geometry and ocean

circulation [e.g., *Duplessy et al*., 1984; *Curry et al*., 1988; *Mix et al*., 1991; *Curry and Oppo*, 2005; *Bostock et al*., 2010; *Knudson and Ravelo*, 2015a]. In the modern ocean, high (low) values of $\delta^{13}C$ of the Dissolved Inorganic Carbon (DIC) are indicative of low (high) nutrient concentrations and large-scale oceanic water mass circulation patterns [*Kroopnick*, 1985]. For $\delta^{13}C$ reconstructions of intermediate- and deep-water mass circulation changes the initial $\delta^{13}C$, which is set in surface waters before subduction into the ocean interior, has to be taken into account. The initial $\delta^{13}C$ value of a water mass is affected by air-sea gas exchange at the surface ocean, which in turn is temperature dependent. After isolation from the surface ocean, the $\delta^{13}C$ of a given water mass is mainly altered by in situ addition of CO_2 through respiration of sinking organic material and mixing with other water masses. Today, a $\delta^{13}C_{DIC}$ of about 1‰ characterize surface waters of the North Atlantic where North Atlantic Deep Water (NADW) is formed. As it flows to the circum-Antarctic Ocean interior the continuous degradation of sinking organic particles reduces the original $\delta^{13}C_{DIC}$ of NADW to about 0.5‰. In the Southern Ocean deep water further recirculates to the Indian and Pacific Oceans and lowest values of ~ −0.6‰ $\delta^{13}C_{DIC}$ are observed today in the deep subarctic Pacific. Since $\delta^{13}C$ of epibenthic foraminifera is closely related to the $\delta^{13}C_{DIC}$ of ambient seawater, past differences in nutrient content and water mass circulation patterns can be reconstructed from benthic foraminiferal tests preserved in marine sediments [e.g., *Duplessy et al*., 1984].

Combined evidence of $\Delta^{14}C$ deep-water ventilation ages and benthic foraminiferal $\delta^{13}C$ records suggest changes in mid-depth circulation (the upper 1000 to ~2000 m water depth) of the North Pacific Ocean under glacial conditions [*Duplessy et al*., 1988; *Herguera et al*., 1992; *Keigwin*, 1998; *Matsumoto et al*., 2002a; *Okazaki et al*., 2012]. Accordingly, the mid-depth circulation of the North Pacific was strengthened by formation of Glacial North Pacific Intermediate Water (GNPIW). In contrast to today, it has been proposed that the Bering Sea formed intermediate waters during glacial times and played an important role in formation of GNPIW [e.g., *Tanaka and Takahashi*, 2005; *Horikawa et al*., 2010]. Evidence for additional cold and well-oxygenated intermediate water in the glacial Bering Sea has been provided from a study based on changes in radiolarian assemblages [*Tanaka and Takahashi*, 2005]. Based on a neodymium isotope record (εNd), it has been argued that Bering Sea intermediate water was a principal component of GNPIW during the glacial period [*Horikawa et al*., 2010]. The formation of glacial Bering Sea intermediate waters was explained by changes in high-latitude hydrological processes such as enhanced brine rejection with the resulting salinity increase favoring the subduction of cold surface waters to the mid-depth in the Bering Sea as important precursor of GNPIW [*Rella et al*., 2012]. A recent study based on endobenthic foraminiferal stable oxygen ($\delta^{18}O$) and $\delta^{13}C$ records from the Bering Sea indicates that enhanced GNPIW formation was not only restricted to the LGM but also recurred during other extreme glacial intervals of the last 1.2 Myr [*Knudson and Ravelo*, 2015a].

There is so far no consensus about the amount of AAIW production during glacial boundary conditions. Based on $\delta^{13}C$ and $\delta^{18}O$ analyses on benthic foraminifera from the Australian margin, it has been suggested that a colder and fresher water mass ventilated at intermediate depths, which was linked to a shift in the frontal zonation within the Southern Ocean [*Lynch-Stieglitz et al*., 1994]. Furthermore, a study based on authigenic minerals from the Chilean margin found higher oxygen concentrations during glacial times, which were linked to an enhanced production of AAIW [*Muratli et al*., 2010]. In contrast, it has been proposed that stronger water column stratification in the Southern Ocean led to a reduced production of AAIW under glacial conditions [*Pahnke and Zahn*, 2005]. Accordingly, periods of increased intermediate water formation were linked to Southern Hemisphere warm episodes through a tight coupling between climate warming and intermediate water production at the high southern latitudes. A recent study combined benthic $\delta^{13}C$ and $\delta^{18}O$ records off New Zealand with modeling results to reconstruct the vertical extent of AAIW over the last 350 kyr [*Ronge et al*., 2015]. These results showed that the vertical extent of AAIW changed on glacial-interglacial timescales with a significantly shallower AAIW subduction under glacial conditions. The shallower subduction of glacial AAIW has been related to an advanced winter sea ice edge as well as enhanced freshwater flux from sea ice melting, which reduced the salinity and resulted in formation of less dense intermediate waters in the Southern Ocean.

Studies based on εNd records as well as $\Delta^{14}C$ shallow- and deep-water ventilation ages from the equatorial Pacific suggest a dominant role of the Southern Ocean in transferring climatic signals from the high latitudes toward the tropical regions during late Marine Isotope Stage (MIS) 2 [*Pena et al*., 2013; *de la Fuente et al*., 2015]. Accordingly, available reconstructions of changes in water mass signatures of the equatorial Pacific suggest

a principal southern source for tropical Pacific intermediate water masses during glacial times similar to today. In a recent study, *Carriquiry et al.* [2015] analyzed $\delta^{13}C$ records at the western Baja California Margin and relates changes in mid-depth nutrient distribution to a larger influence of glacial AAIW to the tropical North Pacific. In contrast, *Leduc et al.* [2010] explained anomalies in glacial $\delta^{13}C$ of intermediate waters in the Eastern Tropical North Pacific (ETNP) by a switch from southern nutrient-poor to northern nutrient-enriched intermediate water masses due to a sustained formation of GNPIW. A recent εNd data compilation from 55 core sites around the Pacific [*Hu et al.*, 2016] revealed a significant offset in EEP εNd signature values between LGM and Holocene values (by 1–2 epsilon units lower than during the Holocene), which has been explained by a higher contribution from northern sourced waters [*Hu et al.*, 2016]. The enhanced penetration of northern sourced water masses is in agreement with evidence for enhanced glacial mid-depth circulation reconstructed from $\delta^{13}C$ records of California margin sediment cores; however, these records also point to spatial and temporal complexity in the ventilation history of the Northeast Pacific [*Stott et al.*, 2000]. Together, these results imply a more prominent role of northern sourced water masses in shaping the mid-depth water mass characteristics of the glacial North Pacific. On the other hand, it still remains illusive how strengthened GNPIW circulation shaped the mid-depth water mass characteristics of the glacial North Pacific and whether GNPIW might have influenced the nutrient distribution, biological productivity, and export patterns far beyond the northern high latitudes.

In this study, we report on stable isotope measurements derived from sedimentary records of the western subarctic Pacific (Bering Sea) and EEP to investigate spatiotemporal changes in GNPIW circulation and its influence on low-latitude Pacific water mass characteristics during the past 60 kyr. We chose a sediment core from the western Bering Sea located on Shirshov Ridge (SO201-2-101KL, 58°52.52′N, 170°41.45′E, 630 m water depth, Figure 1) and measured the $\delta^{13}C$ composition of the epibenthic foraminifera *Cibicides lobatulus* (*C. lobatulus*) as an indicator for past ventilation changes close to the source region of GNPIW [*Max et al.*, 2014]. Today the western Bering Sea is poorly ventilated due to the absence of local intermediate water formation and water masses bathing core site SO201-2-101KL are dominated by upwelling of nutrient-rich PDW (Figure 1b). Additional $\delta^{13}C$ data of deep-dwelling planktonic foraminifera *Globorotaloides hexagonus* (*G. hexagonus*) from Ocean Drilling Program (ODP) Site 1240 (00°01.31′N, 82°27.76′W, 2921 m water depth, Figure 1) provide information about glacial changes of subthermocline water mass characteristics in the EEP. Modern water mass signatures of subthermocline waters at ODP Site 1240 are linked to the lower branch of the EUC, which brings nutrients to the surface ocean of the EEP (Figure 1b). By comparing water mass signatures of intermediate- to deep-water masses of the Pacific Ocean and Southern Ocean with subthermocline to mid-depth water masses in the tropical Pacific we (1) examine whether the influence of northern sourced versus southern sourced water masses on tropical Pacific intermediate and subthermocline water masses of the EEP changed during the last glacial period and (2) discuss potential implications for subthermocline nutrient availability and biological productivity in the equatorial Pacific in the past.

2. Materials and Methods

2.1. Stable Carbon ($\delta^{13}C$) and Oxygen ($\delta^{18}O$) Isotope Measurements From Benthic and Deep-Dwelling Planktonic Foraminifera

We measured the $\delta^{13}C$ and $\delta^{18}O$ isotope composition of epibenthic foraminifera *C. lobatulus* selected from sediment samples of western Bering Sea sediment core SO201-2-101KL and deep-dwelling planktonic foraminifera *G. hexagonus* from samples of ODP Site 1240 in the Panama Basin (Figure 1; see supporting information Tables S1 and S2). Sedimentation rates of 11–16 cm kyr^{-1} have been reported for core SO201-2-101KL from Shirshov Ridge [*Riethdorf et al.*, 2013] and 6.4–25.2 cm kyr^{-1} for ODP Site 1240 [*Pena et al.*, 2008]. According to our sampling scheme, we achieved a millennial to centennial-scale resolution of proxy data in this study with an average temporal resolution of ~ 0.25 kyr for core SO201-2-101KL and ~ 0.23 kyr for the last 60 kyr of ODP Site 1240, respectively. Stable isotope analyses in core SO201-2-101KL were made on samples of two to three specimens of *C. lobatulus* picked from the 250–400 μm size fractions. The stable isotopic composition of *G. hexagonus* of ODP Site 1240 was determined using five specimens per sample picked from the 250–315 μm size fraction.

It has been proposed that *C. lobatulus* preferentially lives attached to hard substrate on or slightly above the sediment surface and studies on living specimen indicated that this species faithfully records the $\delta^{13}C_{DIC}$ of ambient seawater [*Schweizer et al.*, 2009]. Some investigators have observed a positive offset in the $\delta^{13}C$ of *C.*

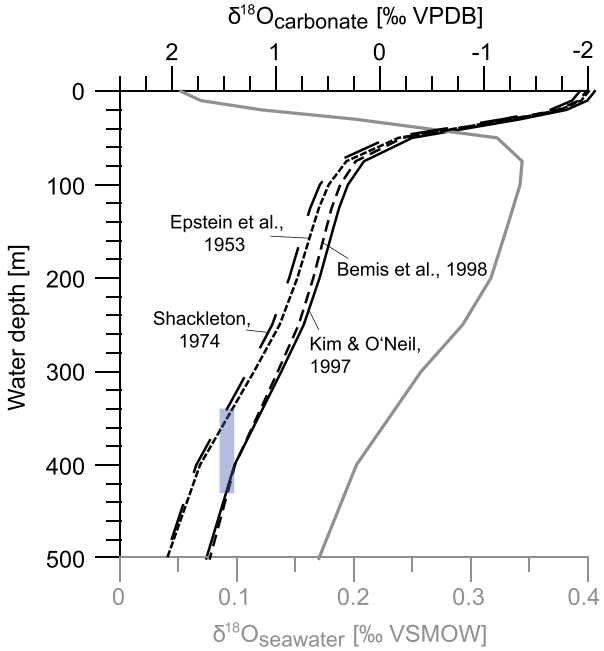

Figure 2. Apparent calcification depth (ACD) of planktonic foraminifera *G. hexagonus* in the Eastern Equatorial Pacific. ACD of *G. hexagonus* at ODP Site 1240 was inferred from best match between measured foraminiferal $\delta^{18}O_{calcite}$ values and corresponding calculated theoretically present $\delta^{18}O_{equilibrium}$ value, which were determined using various paleotemperature equations (black partly dashed lines), modern water temperatures [*Locarnini et al.*, 2010] and $\delta^{18}O_{seawater}$ (gray line). The blue bar indicates the ACD range of *G. hexagonus* considering all used equations.

lobatulus with regard to ambient bottom water $\delta^{13}C_{DIC}$ in some high-latitude settings of the North Atlantic Ocean [*Mackensen et al.*, 2000]. However, this effect was caused by high seasonal variability of the original ambient $\delta^{13}C_{DIC}$-signal, confirmed by time series measurements of water column $\delta^{13}C_{DIC}$ and related to the calcification of *C. lobatulus* during time intervals of maximum ventilation [*Mackensen et al.*, 2000]. We thus regard the $\delta^{13}C$-signal *C. lobatulus* to reliably reflect $\delta^{13}C$ of ambient seawater.

Isotopic compositions of *C. lobatulus* and *G. hexagonus* were measured at the Alfred Wegener Institute, Helmholtz Centre for Polar and Marine Research, Germany, using a Thermo Fisher MAT 253 mass spectrometer coupled to a Kiel IV automatic carbonate preparation device. All stable isotope measurements were calibrated via the NBS-19 international standard, and results are reported in δ notation versus Vienna Peedee belemnite (VPDB) scale. Overall long-term analytical reproducibility of measurements based on internal laboratory standard (Solnhofen limestone) together with samples over a 1 year period is better than $\pm$0.06‰ for $\delta^{13}C$ and $\pm$0.08‰ for $\delta^{18}O$.

2.2. Stable Oxygen Isotope Composition ($\delta^{18}O$) and Apparent Calcification Depth of Deep-Dwelling Planktonic Foraminifera *G. Hexagonus*

Information regarding apparent calcification depth (ACD) of the planktonic foraminifera *G. hexagonus* is still sparse. We make a first attempt to determine the ACD at ODP Site 1240 to validate the depth habitat of *G. hexagonus* in the EEP. The ACD estimation was done by comparing measured foraminiferal $\delta^{18}O_{calcite}$ from a near-core top sample (at 10 cm) to a theoretically expected equilibrium $\delta^{18}O$ values of calcite ($\delta^{18}O_{equilibrium}$) that foraminifera would incorporate in dependence of modern water temperature, salinity, and $\delta^{18}O$ values of seawater ($\delta^{18}O_{seawater}$). In order to calculate $\delta^{18}O_{seawater}$, the $\delta^{18}O_{seawater}$-salinity relationships given by *Leduc et al.* [2007] for 0–40 m water depth,

$$\delta^{18}O_{seawater}(‰) = 0.253\,S\,(\text{p.s.u.}) - 8.52,$$

and for >40 m water depth,

$$\delta^{18}O_{seawater}(‰) = 0.471\,S\,(\text{p.s.u.}) - 16.15$$

were used in conjunction with annual salinity data derived from World Ocean Atlas 2009 [*Antonov et al.*, 2010].

Several established $\delta^{18}O$-paleotemperature equations [*Epstein et al.*, 1953; *Shackleton*, 1974; *Kim and O'Neil*, 1997; *Bemis et al.*, 1998] were considered for $\delta^{18}O_{calcite}$ as absolute ACD estimation strongly depends on the applied temperature equation [*Wejnert et al.*, 2013] (Figure 2). Modern temperatures are derived from the World Ocean Atlas 2009 [*Locarnini et al.*, 2010], and $\delta^{18}O_{seawater}$ were included after correcting $\delta^{18}O_{seawater}$ to the VPDB scale by subtracting the $\delta^{18}O_{seawater}$-conversion factor given in *Bemis et al.* [1998].

The water depth showing the best match between $\delta^{18}O_{calcite}$ and $\delta^{18}O_{equilibrium}$ is taken as the ACD of *G. hexagonus* (Figure 2).

The calculated ACD suggests that *G. hexagonus* dwells below the thermocline in 340–430 m water depth similar to estimated depth habitats defined by *Ortiz et al.* [1996] in the North Pacific. Further support comes from a very recent ACD assessment from the western equatorial Pacific, which concludes that deep-dwelling *G. hexagonus* is a suitable proxy for tracing properties of equatorial subthermocline water masses [*Rippert et al.*, 2016]. Hence, the stable isotopic composition of *G. hexagonus* is considered to reflect the water mass properties of subthermocline waters of the EEP.

2.3. Stratigraphic Approach and Age Models

The stratigraphic framework of western Bering Sea core SO201-2-101KL was constructed using a multiproxy approach described in detail in *Riethdorf et al.* [2013]. Briefly, information derived from high-resolution X-ray fluorescence (XRF) and spectrophotometric logging data (color b*) of core SO201-2-101KL were used for correlation to millennial-scale variability preserved in the North Greenland Ice Core Project (NGRIP) ice core [*Andersen et al.*, 2004] according to the GICC05 timescale [*Svensson et al.*, 2008] (Figure 3a). The tuning of core SO201-2-101KL to NGRIP was further validated by five planktonic radiocarbon ages spanning the time interval from the onset of MIS 2 to the time interval of the last glacial termination (Figure 3a) [see *Max et al.*, 2012].

We adopted the established age scale of ODP Site 1240 described in the work of *Pena et al.* [2008]. The stratigraphic framework of ODP Site 1240 was constructed from 17 accelerator mass spectrometry (AMS) ^{14}C ages based on monospecific samples of the planktonic foraminifera *Neogloboquadrina dutertrei* (*N. dutertrei*) and tuning of the initiation of *N. duterteri* $\delta^{13}C$ minima at ODP Site 1240 to the CO_2 increase in the Vostok CO_2, as shown by *Spero and Lea* [2002]. Graphical correlation of planktonic foraminiferal Mg/Ca derived sea surface temperatures (SST) from ODP Site 1240 to Antarctic Vostok deuterium records was used to get additional age controls for deeper parts of the core (see supplement of *Pena et al.* [2008] for more details) (Figure 3b).

3. Results

The reconstructed glacial (60–20 ka) $\delta^{13}C$ values based on *C. lobatulus* from Bering Sea core SO201-2-101KL show a pronounced variability on millennial timescales, in particular during MIS 3, where they vary between −0.8 and 0.2‰ (Figure 4). Upon millennial-scale variability a long-term trend towards increased $\delta^{13}C$ of Bering Sea intermediate water since the beginning of MIS 3 is clearly visible in core SO201-2-101KL, which culminated during early MIS 2 (~29 ka) with $\delta^{13}C$ signatures of up to ~ 0.3‰ (Figure 4). During MIS 2 $\delta^{13}C$ values show a long-term decrease with $\delta^{13}C$ signatures reaching ~ −0.2‰ at the beginning of the last deglaciation (~17 ka).

During MIS 3 (~60–30 ka) the *G. hexagonus* $\delta^{13}C$ proxy record from ODP Site 1240 indicates the presence of relatively ^{13}C-enriched (nutrient-depleted) water masses with $\delta^{13}C$ signatures of 0.1–0.2‰ and relatively low variability in $\delta^{13}C$ of subthermocline waters (Figure 4). A first switch to relatively ^{13}C-depleted subthermocline water masses in the EEP is apparent during early MIS 2 (~25 ka); the most ^{13}C-depleted values of ~ −0.4‰ are found at the beginning of the last deglaciation (~17 ka).

4. Discussion

Based on our results, we found evidence that the Bering Sea experienced a long-term increase in intermediate water ventilation from the beginning of MIS 3. We also identified most enhanced ventilation of the Bering Sea during MIS 2, which is in accordance with recent results from *Knudson and Ravelo* [2015a]. In general, it confirms previous studies on marine productivity and benthic foraminiferal stable isotope records that imply a long-term increase in $\delta^{13}C$ Bering Sea intermediate water due to local formation of waters masses with lower salinity and higher oxygen content under glacial conditions [*Schlung et al.*, 2013]. *Rella et al.* [2012] argued that an eastward displacement of the Aleutian Low and a shift to predominantly northerly winds over the Bering Sea created favorable conditions for active polynya formation and brine rejection coupled to sea ice formation, which led to intermediate water production as one potential source of GNPIW during the glacial period. A recent study showed that during stadial periods of the deglaciation most of the western Bering Sea was covered by seasonal sea ice [*Méheust et al.*, 2016], thus providing favorable conditions for

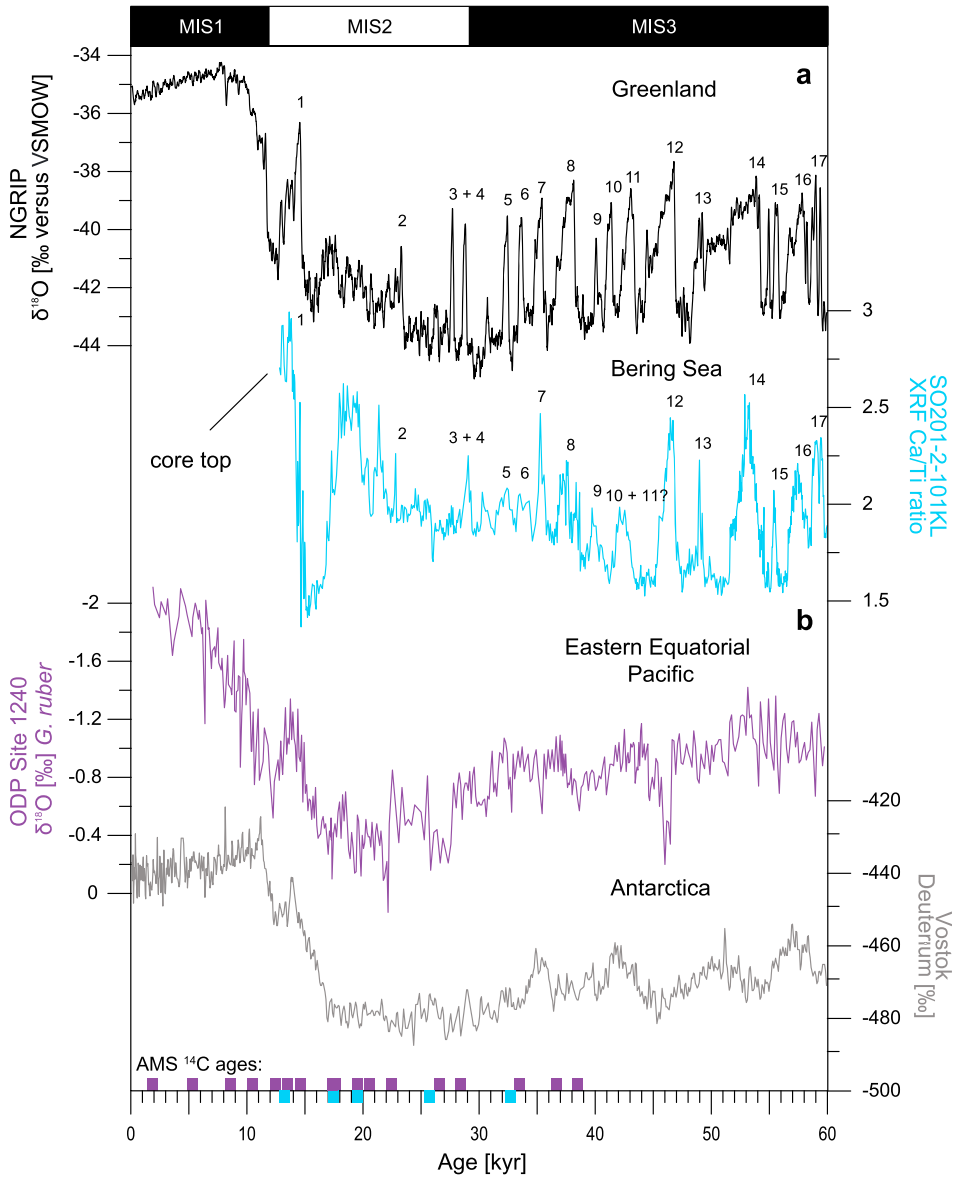

Figure 3. (a) Comparison of high-resolution XRF core-logging data (Ca/Ti ratio) from core SO201-2-101KL to NGRIP ice core record. Numbers indicate Dansgaard-Oeschger Interstadials in NGRIP [*Andersen et al.*, 2004] and SO201-2-101KL (this study) during the past 60 kyr [*Riethdorf et al.*, 2013]. (b) The stratigraphic framework of ODP Site 1240 based on 17 AMS ^{14}C ages and graphical tuning of deeper parts of the cores to the Vostok ice core record [*Petit et al.*, 1999; *Pena et al.*, 2008]. Available AMS ^{14}C datings derived from core SO201-2-101KL and ODP Site 1240 are given by blue and purple squares at the bottom.

intermediate water formation. Moreover, benthic δ^{13}C data from proximal core SO201-2-85KL point to a decline in δ^{13}C and reduced ventilation during deglacial warm stages and the early Holocene when sea ice cover was substantially reduced [*Max et al.*, 2012; *Max et al.*, 2014]. However, changes in thermodynamic (temperature-dependent) equilibration between the surface ocean $\delta^{13}C_{DIC}$ and the atmospheric CO_2 also influence isotopic fractionation, whereby surface ocean $\delta^{13}C_{DIC}$ increases by 0.1‰ with each 1°C decrease in surface ocean temperature [*Mook et al.*, 1974]. Given that glacial production of intermediate waters in the western Bering Sea was supposedly linked to sea ice formation during winter, when surface ocean temperature were always close to the freezing point, temperature-dependent changes in air-sea gas exchange of western Bering Sea surface waters should have had a minor effect on the $\delta^{13}C_{DIC}$ signal.

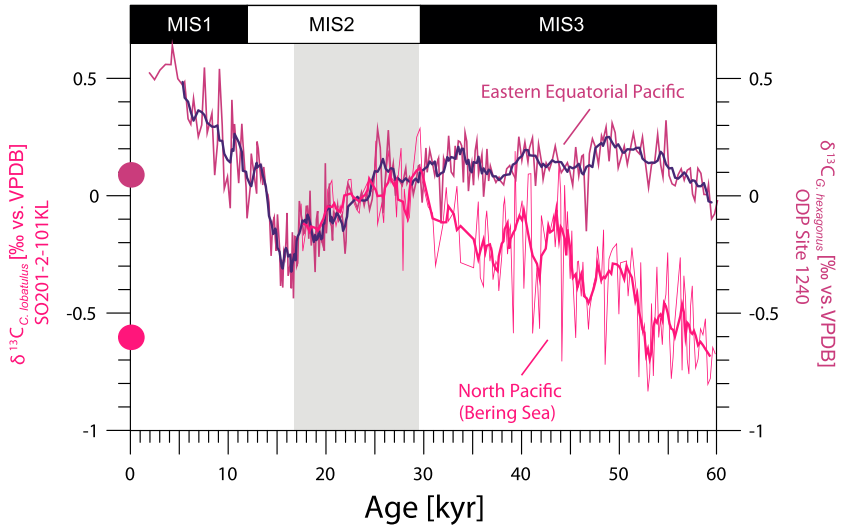

Figure 4. Detailed comparison of mid-depth benthic $\delta^{13}C$ record from sediment core SO201-2-101KL from the subarctic Pacific (Bering Sea) with $\delta^{13}C$ record of deep-dwelling (subthermocline) planktonic foraminifera *G. hexagonus* derived from ODP Site 1240 in the Eastern Equatorial Pacific during the past 60 kyr. Gray shaded area marks times of convergence between the given $\delta^{13}C$ records during MIS 2. Colored circles indicate $\delta^{13}C_{DIC}$ composition of water masses bathing the respective core sites under modern conditions [*Key et al.*, 2004].

4.1. Glacial Contribution of Northern Versus Southern Sourced Water Masses in the Eastern Tropical North Pacific (~8°N)

To assess the influence of northern versus southern sourced water masses on EqPIW characteristics during the past 60 kyr, we compare benthic $\delta^{13}C$ mid-depth records from the subarctic Pacific (SO201-2-101KL; this study) and the Southern Ocean (SO213-84-1 [*Ronge et al.*, 2015]) as well as a deep-water benthic $\delta^{13}C$ record from the Northeast Pacific (W8709A-13PC [*Lund and Mix*, 1998]) with mid-depth $\delta^{13}C$ signatures derived from sediment core MD02-2529 [*Leduc et al.*, 2010] located in the ETNP (Figures 1 and 5a). The core site of MD02-2529 in the ETNP is situated at the modern confluence of northern oxygen-poor and southern oxygen-rich waters and thus is ideally located to investigate past changes in the respective latitudinal extents of northern versus southern sourced water masses in the past [*Leduc et al.*, 2010].

First, we consider our new benthic $\delta^{13}C$ record from the mid-depth subarctic Pacific (SO201-2-101KL) and the benthic $\delta^{13}C$ record of PDW from the Northeast Pacific (W8709A-13PC) [*Lund and Mix*, 1998], which are compared with EqPIW $\delta^{13}C$ water mass characteristics (MD02-2529) [*Leduc et al.*, 2010] during the past 60 kyr (Figures 1 and 5a). Millennial-scale variability superimposed on the long-term $\delta^{13}C$ trend of EqPIW is more pronounced compared to the $\delta^{13}C$-signal recorded in SO201-2-101KL (GNPIW) or W8709A-13PC (PDW) during early MIS 3 (55–45 ka). In addition EqPIW $\delta^{13}C$ values oscillate between $\delta^{13}C$ signatures of GNPIW and PDW during MIS 3 (60–30 ka). During this time, there is no clear relationship to northern or southern sourced intermediate waters, and rather, admixing of different source water masses to EqPIW is likely. On the other hand, clear similarities in the long-term evolution in $\delta^{13}C$ between the intermediate water records derived from subarctic Pacific core SO201-2-101KL and sediment core MD02-2529 from the ETNP are observed since at least ~ 29 ka (Figure 5a). Moreover, glacial gradients in $\delta^{13}C$ between GNPIW and EqPIW are relatively small and vary between 0.2 and 0.5‰. In contrast, absolute $\delta^{13}C$ signatures as well as the temporal evolution of EqPIW and PDW differs substantially such as $\delta^{13}C$ of EqPIW increases steadily, whereas $\delta^{13}C$ of PDW shows a long-term trend to more depleted ^{13}C signatures during MIS 2 (Figure 5a). Accordingly, available deep-water ventilation ages as well as the long-term trend in deep-water $\delta^{13}C$ of the North Pacific indicate that glacial PDW was similar or even less well ventilated than today [*Lund and Mix*, 1998; *Galbraith et al.*, 2007; *Lund et al.*, 2011] and the ventilation history different to the mid-depth circulation dynamics of the North Pacific [*Kennett and Ingram*, 1995; *Stott et al.*, 2009]. Altogether, our results indicate that intermediate waters in the subarctic Pacific and ETNP (GNPIW and EqPIW) share similar glacial $\delta^{13}C$ signatures, which are indicative for the presence of nutrient-enriched intermediate water masses but are apparently different to $\delta^{13}C$ signatures

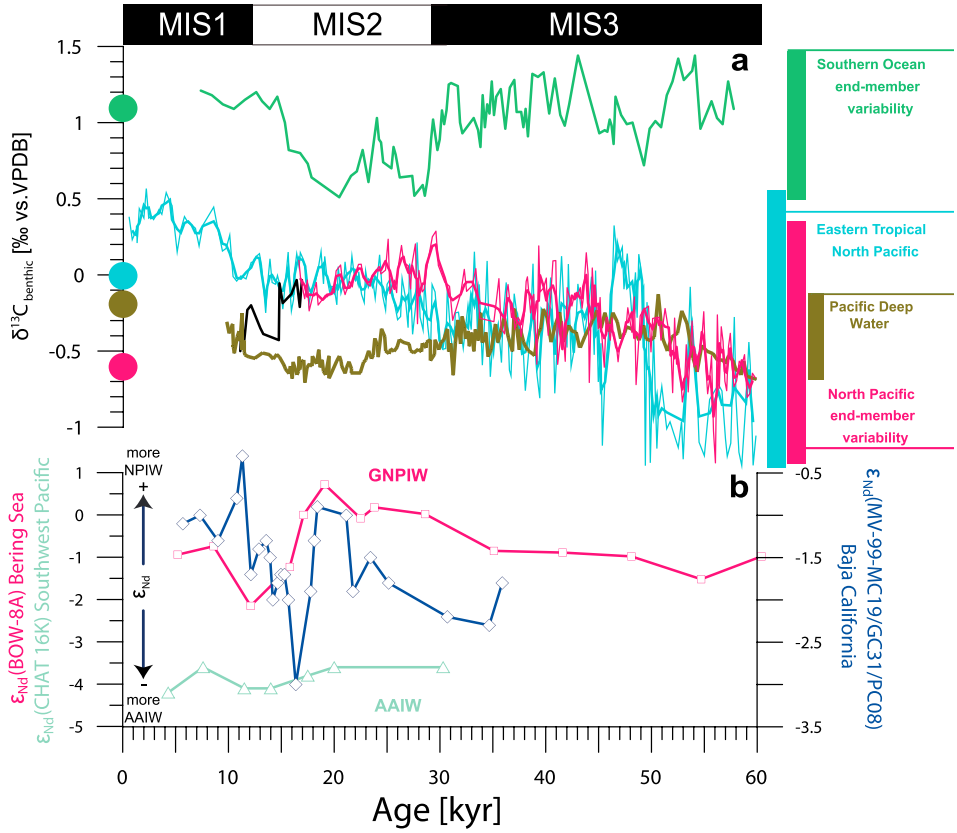

Figure 5. Benthic $\delta^{13}C$ records and εNd signatures from intermediate waters of the North Pacific (GNPIW), off Baja California, the Eastern Tropical North Pacific (EqPIW), and the Southern Ocean (AAIW) compared to benthic $\delta^{13}C$ deep-water (PDW) variability for the last 60 kyr. (a) Benthic $\delta^{13}C$ record from Southern Ocean core SO213-84-1 (AAIW, in green) [*Ronge et al.*, 2015], benthic $\delta^{13}C$ record from MD02-2529 located in the Eastern Tropical North Pacific (in light blue) [*Leduc et al.*, 2010], benthic intermediate-water $\delta^{13}C$ record from Bering Sea core SO201-2-101KL (in magenta; this study) and SO201-2-85KL (in black) [*Max et al.*, 2014], and deep-water benthic $\delta^{13}C$ record from core W8709A-13PC (in brown) [*Lund and Mix*, 1998]. (b) End-member intermediate-water mass εNd records from southern Bering Sea core BOW-8A (GNPIW, in magenta) [*Horikawa et al.*, 2010] and Southwest Pacific core CHAT 16K (AAIW, in light green) [*Noble et al.*, 2013] together with εNd signatures derived from sediment cores off Baja California (in blue) [*Basak et al.*, 2010]. Colored vertical bars indicate total variability in measured $\delta^{13}C$ at respective core sites. Colored circles indicate $\delta^{13}C_{DIC}$ composition of water masses bathing respective core sites under modern conditions [*Key et al.*, 2004].

of PDW (Figure 5a). Given that GNPIW features slightly higher $\delta^{13}C$ signatures compared to EqPIW masses, our results point to the advection of northern sourced intermediate water masses towards the tropical Pacific. Thus, from similarities in long-term evolution of $\delta^{13}C$ between the North Pacific and ETNP intermediate water records, we argue that relatively nutrient-enriched GNPIW generally extended farther south to the tropical Pacific under glacial conditions. During the last deglaciation (~17–15 ka), however, intermediate water $\delta^{13}C$ signals at the ETNP and North Pacific starts to diverge substantially. The $\delta^{13}C$ signatures in the ETNP increase, while the $\delta^{13}C$ values decrease at site SO201-2-85KL in the subarctic Pacific (Figure 5a).

The glacial $\delta^{13}C$ end-member variability of AAIW is reflected by sediment core SO213-84-1 off New Zealand, where glacial $\delta^{13}C$ signatures of AAIW vary between ~ 0.5 and 1.4‰ [*Ronge et al.*, 2015] (Figure 5a). The long-term evolution of $\delta^{13}C$ signatures between AAIW and intermediate waters in the North Pacific and ETNP reveals remarkable differences in temporal variability under glacial conditions (Figure 5a). Moreover, huge gradients in $\delta^{13}C$ (up to 2‰) between Southern Ocean core SO213-84-1 and MD02-2529 from the ETNP [*Leduc et al.*, 2010] clearly separate ^{13}C-enriched (more nutrient-depleted) signatures of AAIW from ^{13}C-depleted (more nutrient-enriched) signatures of EqPIW under glacial conditions (Figure 5a). Evidence for a weakened production or shoaling of glacial AAIW has been inferred from $\delta^{13}C$ records off New Zealand [*Pahnke and Zahn*, 2005; *Ronge et al.*, 2015], which generally points to a glacial change in relative contribution

of intermediate waters from the Southern Ocean to the tropical Pacific. Thus, large gradients and the discrepancy in temporal evolution of $\delta^{13}C$ signatures of EqPIW and AAIW are indicative for additional water masses influencing the glacial mid-depth tropical Pacific.

Independent evidence for enhanced glacial influence of northern sourced intermediate waters to the low-latitude Pacific comes from the comparison of available εNd records of the Bering Sea and off Baja California [*Basak et al*., 2010; *Horikawa et al*., 2010] (Figure 5b). In particular, εNd data at the intermediate depth in the Bering Sea show radiogenic values explicitly indicating that Bering Sea surface water masses (marked by more radiogenic εNd signatures) were subducted to intermediate depths under glacial conditions [*Horikawa et al*., 2010]. At the same time, glacial εNd values derived from a sediment record off Baja California point to the presence of more radiogenic intermediate water masses, which has been linked to admixture of dominantly northern sourced intermediate waters [*Basak et al*., 2010]. Furthermore, available information of glacial εNd signatures from a sediment core in the Southwest Pacific [*Noble et al*., 2013] clearly distinguish less radiogenic εNd signatures of AAIW from signals of more radiogenic intermediate water masses found in the Bering Sea or off Baja California (Figure 5b). Altogether, results from εNd records are in line with enhanced glacial advection of northern sourced intermediate water masses towards the tropical Pacific (Figures 1 and 5b). However, rapid changes in Bering Sea and Baja California εNd signatures are visible during the last deglaciation that point to a switchback to reduced influence of northern sourced intermediate water masses to the low-latitude Pacific since ~ 17 ka (Figure 5b).

The combined evidences from $\delta^{13}C$ and εNd proxy data of the subarctic Pacific, the eastern North Pacific (Baja California), the ETNP, and Southern Ocean suggest that northern sourced intermediate waters extended farther south to the ETNP under glacial conditions (Figures 5a and 5b). This is in agreement with a scenario proposed by *Herguera et al.* [2010], in which a deepening of the main thermocline and cooling of the high-latitude North Pacific would lead to a southeastward expansion of GNPIW circulation and greater glacial influence of northern sourced intermediate water on the tropical Pacific. Therefore, we propose that glacial changes in the relative contribution of intermediate waters from both the Southern Ocean and North Pacific are important in recirculating excess nutrients from the high-latitude oceans toward the low-latitude regions of the Pacific Ocean. We suggest that the observed glacial changes in $\delta^{13}C$ signatures of tropical intermediate waters in the ETNP are linked to additional contribution of northern sourced intermediate waters that further confirm considerations of a southward expansion of GNPIW to explain the $\delta^{13}C$ signatures found in the mid-depth tropical Pacific during MIS 2 [*Herguera et al*., 2010].

4.2. Evidence for Increased GNPIW Influence on the Eastern Equatorial Pacific Since MIS 2?

To assess whether GNPIW expanded farther south to the equatorial upwelling system, we compare the variability in $\delta^{13}C$ of GNPIW and AAIW with our new subthermocline $\delta^{13}C$ proxy record of the deep-dwelling planktonic foraminifera *G. hexagonus* from ODP Site 1240. Glacial variations in $\delta^{13}C$ of subthermocline water masses are interpreted as both changes in incoming nutrients and export productivity in the surface ocean of the EEP. During MIS 3 (~60–30 ka) the *G. hexagonus* $\delta^{13}C$ proxy record indicates the presence of relatively ^{13}C-enriched (nutrient-depleted) water masses with low variability in $\delta^{13}C$ of subthermocline waters of the EEP (Figure 6a). At the same time, GNPIW shows distinctly lower (more nutrient-rich) $\delta^{13}C$ values with higher temporal variability than EEP subsurface waters. However, apparent similarities are observed since ~ 29 ka at the beginning of MIS 2, where absolute $\delta^{13}C$ values as well as the long-term trend indicate more nutrient-enriched subthermocline water masses recorded in $\delta^{13}C$ of *G. hexagonus* at ODP Site 1240, which closely follows the temporal evolution of the $\delta^{13}C$ signature advected towards the tropical Pacific via GNPIW (Figure 6a).

Interestingly, another rapid switch to monotonically increasing $\delta^{13}C$ of *G. hexagonus* is visible during the last deglaciation, which suggests a decoupling from northern sourced intermediate waters between ~ 17 and 15 ka. The transition from ^{13}C-depleted (more nutrient-enriched) to rather ^{13}C-enriched (more nutrient-depleted) subsurface water implies another significant change in characteristics of source water masses along with changes in biological productivity in the EEP during the last deglaciation (Figures 6a and 6b). Simultaneously, intermediate waters in the North Pacific became further ^{13}C-depleted and seem to be decoupled from subthermocline waters in the EEP. This is in line with a study on surface ocean productivity at ODP Site 1240, which showed that southern sourced intermediate waters played a more dominant role for the nutrient redistribution in the EEP since the early deglaciation [e.g., *Calvo et al*., 2011]. Dissimilar trends are

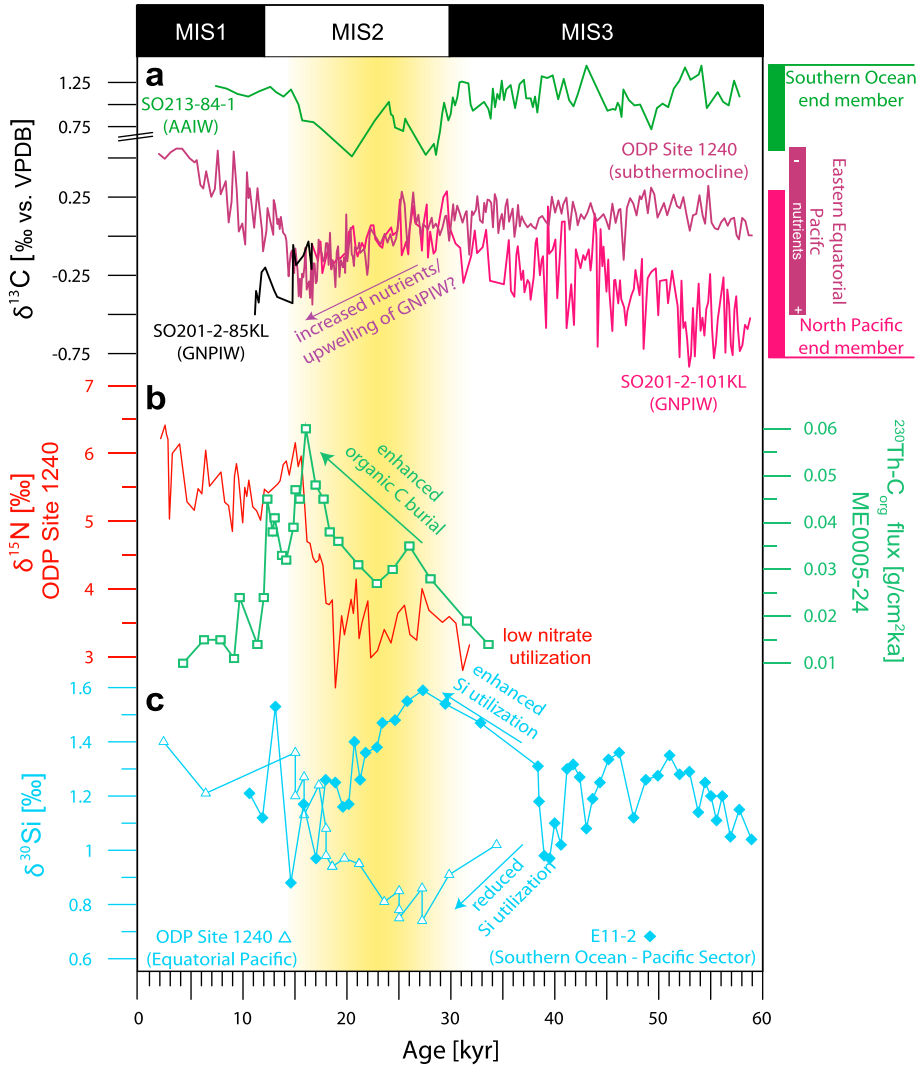

Figure 6. Reconstructed $\delta^{13}C$ variability of GNPIW versus AAIW compared to glacial changes in $\delta^{13}C$ of subthermocline waters, biological productivity, and nutrient utilization in the Eastern Equatorial Pacific (EEP) and Southern Ocean. (a) $\delta^{13}C$ record of GNPIW (SO201-2-85KL [*Max et al.*, 2014]; SO201-2-101KL (this study)) compared to $\delta^{13}C$ composition of AAIW (SO213-84-1 [*Ronge et al.*, 2015]) and deep-dwelling planktonic foraminifera $\delta^{13}C$ record of *G. hexagonus* (ODP Site 1240, this study) during the past 60 kyr. (b) $\delta^{15}N$ record at ODP Site 1240 in the EEP [*Pichevin et al.*, 2009] together with ^{230}Th-normalized C_{org} flux of neighboring core ME0005-24 [*Kienast et al.*, 2007]. (c) $\delta^{30}Si_{Diatom}$ isotope composition of ODP Site 1240 in the EEP [*Pichevin et al.*, 2009] compared to $\delta^{30}Si_{Diatom}$ composition derived from core E11-2 [*Robinson et al.*, 2014] located in the Pacific Zone of the Southern Ocean. Yellow shaded bar marks times of increased GNPIW contribution to subthermocline waters of the EEP during MIS 2.

also evident between northern sourced intermediate water and mid-depth water masses in the ETNP, probably due to a reduced lateral extent of GNPIW during the last deglaciation (Figure 5a). Since then, mid-depth waters in the ETNP seem to follow the temporal variability of southern sourced intermediate water that imply a larger influence of ^{13}C-enriched (more nutrient-depleted) AAIW in the tropical Pacific. However, we note that large gradients between $\delta^{13}C$ of subthermocline waters in the EEP and AAIW are also present during the last deglaciation and Holocene. Still, available benthic $\delta^{13}C$ records from the mid-depth to deep North Pacific do not cover the whole Holocene and impede further interpretation of $\delta^{13}C$ variability in the ETNP during this time.

Past changes in subthermocline water mass signatures in the EEP have been usually linked to differences in advection and/or source water mass characteristics of Southern Ocean water masses to the tropical Pacific. Rapid changes in meridional transport of southern sourced intermediate water toward the tropical regions

have been proposed from εNd records over the last 30 kyr [*Pena et al*., 2013]. A recent study investigating Southern Ocean and EEP shallow- and deep-water ventilation ages suggest that relatively old water masses (PDW/UCDW) upwelled to EEP thermocline waters and proposed a dominant deep southern source during late MIS 2 [*de la Fuente et al*., 2015]. A study reconstructing radiocarbon activity of mid-depth waters from sediment cores off Baja California also pointed to the presence of slightly older intermediate waters in the eastern North Pacific during the latter part of the glacial period [*Marchitto et al*., 2007], which might also explain glacial age anomalies in the surface ocean of the EEP. Thus, we explain changes in $\delta^{13}C$ of subthermocline water masses of the EEP between MIS 3 and MIS 2 by changes in source water mass characteristics probably due to variable ocean interior transport pathways reaching the equatorial Pacific under glacial conditions. Based on the apparent similarities between $\delta^{13}C$ signatures of northern sourced intermediate waters, mid-depth waters in the Panama basin of the ETNP and subthermocline waters in the EEP (Figures 5a and 6a), we argue for additional intrusion of GNPIW into subthermocline water masses of the EEP during MIS 2.

4.3. "North Pacific Nutrient Leakage"

We provide the first evidence that relatively ^{13}C-depleted (nutrient-enriched) GNPIW influenced glacial EEP subthermocline waters during MIS 2 and discuss further potential implications on marine productivity of the equatorial Pacific regions at that time (Figures 6a–6c). Nitrogen and silicon isotopes are often used as diagnostic tools for reconstructing past nutrient cycling. With higher nutrient consumption, both substrate (dissolved nutrients) and products generated from it become progressively enriched in heavier isotopes [*Robinson et al*., 2014]. Indeed, several studies of sediment cores in the EEP found evidence for changes in marine productivity and nutrient utilization during MIS 2 [*Kienast et al*., 2007; *Pichevin et al*., 2009; *Robinson et al*., 2009; *Dubois et al*., 2011] (Figure 6b). Overall similarities between these records demonstrate that they are not primarily influenced by local processes at the deposition site but rather reflect a robust signal of regional changes in nutrient delivery and biological productivity in the EEP [*Dubois et al*., 2011]. *Pichevin et al.* [2009] suggested that the glacial biological carbon pump in the EEP was more efficient due to a relaxation of nutrient limitation and speculated about its contribution to lower atmospheric CO_2 conditions during MIS 2.

Glacial relaxation of nutrient limitation and concurrent maxima in biological productivity in the EEP have been usually related to the redistribution of excess nutrients (mainly silicic acid) from the Southern Ocean via ocean tunneling as proposed by the Silicic Acid Leakage Hypothesis [*Matsumoto et al*., 2002b]. At the same time, changes in the contribution of northern sourced intermediate waters are often neglected, e.g., by assuming that the relative contribution from northern and southern sourced water did not change significantly in the past [e.g., *Dubois et al*., 2011; *Pena et al*., 2013]. However, studies using diatom-bound silicon and nitrogen isotopes as proxies for nutrient utilization suggested enhanced glacial drawdown of silicic acid and nitrate along with higher glacial opal fluxes in the Pacific Subantarctic Zone of the Southern Ocean during MIS 2 [*Bradtmiller et al*., 2009; *Robinson et al*., 2005, 2014]. These results show that in contrast to the EEP, silicic acid and nitrate have been utilized more efficiently and became rather "trapped" north of the Antarctic Polar Front in the glacial deep Southern Ocean (Figures 6b and 6c). However, it has been also shown that average glacial opal fluxes were less than during the Holocene south of the Antarctic Polar Front [*Bradtmiller et al*., 2009]. Whether the glacial Southern Ocean provides sufficient nutrients via ocean tunneling to enhance marine productivity at the EEP as predicted by the Silicic Acid Leakage Hypothesis is still controversial [*Hendry and Brzezinski*, 2014*; Robinson et al*., 2014].

Interestingly, times of enhanced organic carbon flux rates and low nutrient utilization (silicic acid and nitrate) in the EEP are visible since the beginning of MIS 2 and generally coincided with the proposed changes in additional contributions of relatively nutrient-rich GNPIW to equatorial Pacific subthermocline water masses (Figures 6b and 6c). Invoking an additional export of unutilized (preformed) nutrients from the high-latitude North Pacific via nutrient-enriched GNPIW (here named as "North Pacific Nutrient Leakage") thus might be another, yet unconsidered, process to explain relieved nutrient limitation and a stimulated biological pump in the EEP during MIS 2. Unfortunately, less is known about glacial changes in utilization of major nutrients, such as silicon or iron in the source region of GNPIW. Some studies propose low biological productivity and nutrient utilization (nitrate) in the Bering Sea due to a decrease in productivity, or an increase in nitrate availability through changes in vertical mixing under glacial conditions [*Riethdorf et al*., 2013; *Schlung et al*., 2013]. Other studies point to near-complete nutrient utilization (nitrate) in the Bering Sea and western subarctic

Pacific during glacial times [*Brunelle et al*., 2007, 2010]. A recent study emphasizes the role of strong physical stratification of the glacial subarctic Pacific surface waters, which prevented additional flux of nitrate from underlying water, such that available surface nitrate was used to near completion [*Knudson and Ravelo*, 2015b]. Our results propose that additional influence of nutrient-rich North Pacific mid-depth waters to the tropical Pacific via GNPIW might hold new clues about glacial productivity changes in the EEP but need to be further evaluated in order to understand the role of enhanced influence of GNPIW to the low-latitude Pacific under glacial conditions.

During the deglaciation, the resumption of intense overturning within the Southern Ocean led to a higher injection of relatively nutrient-depleted southern sourced water masses into the EqPIW. As a consequence, decreasing nutrient concentrations and increasing nutrient consumption are recorded in the EqPIW (Figure 6). However, we can only speculate about the offset in timing between the onset of EqPIW $\delta^{13}C$ changes (shown by *G. hexagonus*) and the increase in $\delta^{15}N$ in ODP Site 1240. The switch in relative end-member contribution during the deglaciation possibly causes variations in intermediate water suboxia and hence water column denitrification [*Robinson et al*., 2009]. This would affect the nitrogen isotopes only as *G. hexagonus* seems to be more insensitive to varying oxygen concentrations [*Rippert et al*., 2016]. Nonetheless, the discrepancy in timing needs to be further investigated in combination with $\delta^{15}N$ studies from the subarctic Pacific.

5. Conclusions

Here we report on new foraminiferal $\delta^{13}C$ records from the western subarctic Pacific (Bering Sea) and EEP spanning the past 60 kyr. Combined evidence of $\delta^{13}C$ from core SO201-2-101KL and εNd records of the Bering Sea points to a long-term increase in GNPIW formation since the onset of MIS 3, which culminated early in MIS 2 (~29 ka). The comparison between benthic foraminiferal $\delta^{13}C$ records of SO201-2-101KL and marine sediment core MD02-2529 from the Panama Basin as well as εNd records of the Bering Sea and eastern North Pacific reveals remarkable similarities in the long-term evolution between GNPIW and EqPIW signatures in the tropical North Pacific during the glacial period. These results support the notion that northern sourced intermediate water extended farther south to the tropical Pacific region than today under glacial boundary conditions. Glacial changes in $\delta^{13}C$ of subthermocline water masses in the EEP were derived from deep-dwelling planktonic foraminiferal species *G. hexagonus* at ODP Site 1240 and indicate significant changes in subthermocline water mass characteristics during MIS 2. Notably, the proposed times of additional influence of GNPIW to the tropical Pacific coincides with changes in nutrient availability and biological productivity in the glacial EEP. Overall, our new findings indicate that past changes in North Pacific mid-depth circulation might have played a crucial role in glacial nutrient availability and biological productivity in the EEP but needs to be further constrained by future studies investigating glacial changes in utilization of major nutrients, such as silicon or iron in the subarctic Pacific.

Acknowledgments

The Helmholtz Climate Initiative REKLIM (Regional climate change) funded this study. N.R., L.L.J., and R.T. received funding through research projects Manihiki II (03G0225B) and SiGePAX (03F0704A) by the Bundesministerium für Bildung und Forschung (BMBF). This research used samples provided by BMBF-project KALMAR and the International Ocean Discovery Program (IODP). IODP was sponsored by the U.S. National Science Foundation (NSF) and participating countries under the management of Joint Oceanographic Institutions (JOI), Inc. We gratefully acknowledge the Master and crew of R/V *SONNE* cruises SO201-2 (KALMAR) and thank for their professional support on board. We express our thanks to L. Schönborn and G. Meyer for conducting stable isotope measurements at the AWI stable isotope lab. The authors thank Isabel Cacho and Helen Bostock for helpful comments and suggestions. We also would like to thank the anonymous reviewer, who helped to improve the quality of this manuscript. Supplementary data are available at PANGAEA - Data Publisher for Earth & Environmental Science (https://doi.org/10.1594/PANGAEA.869243).

References

Andersen, K. K., et al. (2004), High-resolution record of Northern Hemisphere climate extending into the last interglacial period, *Nature*, *431*, 147–151.

Antonov, J. I., D. Seidov, T. P. Boyer, R. A. Locarnini, A. V. Mishonov, H. E. Garcia, O. K. Baranova, M. M. Zweng, and D. R. Johnson (2010), in *World Ocean Atlas 2009, Volume 2: Salinity*, *NOAA Atlas NESDIS*, vol. 69, edited by S. Levitus, pp. 184, U.S. Gov. Print. Off., Washington D. C.

Basak, C., E. E. Martin, K. Horikawa, and T. M. Marchitto (2010), Southern Ocean source of superset of ^{14}C-depleted carbon in the North Pacific Ocean during the last deglaciation, *Nat. Geosci.*, *3*(11), 770–773.

Bemis, B. E., H. J. Spero, J. Bijma, and D. W. Lea (1998), Reevaluation of the oxygen isotopic composition of planktonic foraminifera: Experimental results and revised paleotemperature equations, *Paleoceanography*, *13*, 150–160, doi:10.1029/98PA00070.

Bostock, H. C., B. N. Opdyke, and M. J. M. Williams (2010), Characterising the intermediate depth waters of the Pacific Ocean using $\delta^{13}C$ and other geochemical tracers, *Deep Sea Res., Part I*, *57*(7), 847–885.

Bradtmiller, L. I., R. F. Anderson, M. Q. Fleisher, and L. H. Burckle (2009), Comparing glacial and Holocene opal fluxes in the Pacific sector of the Southern Ocean, *Paleoceanography*, *24*, PA2214, doi:10.1029/2008PA001693.

Brunelle, B. G., D. M. Sigman, M. S. Cook, L. D. Keigwin, G. H. Haug, B. Plessen, G. Schettler, and S. L. Jaccard (2007), Evidence from diatom-bound nitrogen isotopes for subarctic Pacific stratification during the last ice age and a link to North Pacific denitrification changes, *Paleoceanography*, *22*, PA1215, doi:10.1029/2005PA001205.

Brunelle, B. G., D. M. Sigman, S. L. Jaccard, L. D. Keigwin, B. Plessen, G. Schettler, M. S. Cook, and G. H. Haug (2010), Glacial/interglacial changes in nutrient supply and stratification in the western subarctic North Pacific since the penultimate glacial maximum, *Quat. Sci. Rev.*, *29*, 2579–2590.

Calvo, E., C. Pelejero, L. D. Pena, I. Cacho, and G. A. Logan (2011), Eastern Equatorial Pacific productivity and related-CO_2 changes since the last glacial period, *Proc. Natl. Acad. Sci. U.S.A.*, *108*, 5537–5541.

Carriquiry, J. E. D., A. Sanchez, and G. Leduc (2015), Southern Ocean influence on the Eastern Tropical North Pacific's intermediate depth circulation during the last glacial maximum, *Paleoceanography*, *30*, 1132–1151, doi:10.1002/2014PA002766.

Curry, W. B., and D. W. Oppo (2005), Glacial water mass geometry and the distribution of $\delta^{13}C$ of Sigma CO_2 in the western Atlantic Ocean, *Paleoceanography*, *20*, PA1017, doi:10.1029/2004PA001021.

Curry, W. B., J. C. Duplessy, L. D. Labeyrie, and N. J. Shackleton (1988), Changes in the distribution of $\delta^{13}C$ of deep water Sigma CO_2 between the last glaciation and the Holocene, *Paleoceanography*, *3*, 317–341, doi:10.1029/PA003i003p00317.

de la Fuente, M., L. Skinner, E. Calvo, C. Pelejero, and I. Cacho (2015), Increased reservoir ages and poorly ventilated deep waters inferred in the glacial Eastern Equatorial Pacific, *Nat. Commun.*, *6*, 7420, doi:10.1038/ncomms8420.

Dubois, N., M. Kienast, S. Kienast, C. Normandeau, S. E. Calvert, T. D. Herbert, and A. Mix (2011), Millennial-scale variations in hydrography and biogeochemistry in the Eastern Equatorial Pacific over the last 100 kyr, *Quat. Sci. Rev.*, *30*, 210–223.

Dugdale, R. C., A. G. Wischmeyer, F. P. Wilkerson, R. T. Barber, F. Chai, M. S. Jiang, and T. H. Peng (2002), Meridional asymmetry of source nutrients to the equatorial Pacific upwelling ecosystem and its potential impact on ocean–atmosphere CO(2) flux: A data and modeling approach, *Deep Sea Res., Part II*, *49*, 2513–2531.

Duplessy, J. C., N. J. Shackleton, R. G. Fairbanks, L. Labeyrie, D. Oppo, and N. Kallel (1988), Deepwater source variations during the last climatic cycle and their impact on the global deepwater circulation, *Paleoceanography*, *3*, 343–360, doi:10.1029/PA003i003p00343.

Duplessy, J. C., N. J. Shackleton, R. K. Matthews, W. Prell, W. F. Ruddiman, M. Caralp, and C. H. Hendy (1984), C-13 record of benthic foraminifera in the last interglacial ocean—Implications for the carbon-cycle and the global deep-water circulation, *Quat. Res.*, *21*, 225–243.

Epstein, S., R. H. Buchsbaum, A. Lowenstam, and H. C. Urey (1953), Revised carbonate-water isotopic temperature scale, *Geol. Soc. Am. Bull.*, *64*, 1315–1325.

Galbraith, E. D., S. L. Jaccard, T. F. Pedersen, D. M. Sigman, G. H. Haug, M. Cook, J. R. Southon, and R. Francois (2007), Carbon dioxide release from the North Pacific abyss during the last deglaciation, *Nature*, *449*, 890–894.

Garcia, H. E., R. A. Locarnini, T. P. Boyer, J. I. Antonov, M. M. Zweng, O. K. Baranova, and D. R. Johnson (2010), In *World Ocean Atlas 2009, Volume 4: Nutrients (Phosphate, Nitrate, Silicate)*, *NOAA Atlas NESDIS*, vol. 71, edited by S. Levitus, pp. 398, U.S. Gov. Print. Off., Washington, D. C.

Haug, G. H., D. M. Sigman, R. Tiedemann, T. F. Pedersen, and M. Sarnthein (1999), Onset of permanent stratification in the subarctic Pacific Ocean, *Nature*, *401*(6755), 779–782.

Hendry, K. R., and M. A. Brzezinski (2014), Using silicon isotopes to understand the role of the Southern Ocean in modern and ancient biogeochemistry and climate, *Quat. Sci. Rev.*, *89*, 13–26.

Herguera, J. C., E. Jansen, and W. H. Berger (1992), Evidence for a bathyal front at 2000-M depth in the glacial Pacific, based on a depth transect on Ontong Java Plateau, *Paleoceanography*, *7*, 273–288, doi:10.1029/92PA00869.

Herguera, J. C., T. Herbert, M. Kashgarian, and C. Charles (2010), Intermediate and deep water mass distribution in the Pacific during the Last Glacial Maximum inferred from oxygen and carbon stable isotopes, *Quat. Sci. Rev.*, *29*, 1228–1245.

Honda, M. C., K. Imai, Y. Nojiri, F. Hoshi, T. Sugawara, and M. Kusakabe (2002), The biological pump in the northwestern North Pacific based on fluxes and major components of particulate matter obtained by sediment-trap experiments (1997–2000), *Deep Sea Res., Part II*, *49*, 5595–5625.

Horikawa, K., Y. Asahara, K. Yamamoto, and Y. Okazaki (2010), Intermediate water formation in the Bering Sea during glacial periods: Evidence from neodymium isotope ratios, *Geology*, *38*, 435–438.

Hu, R., A. M. Piotrowski, H. C. Bostock, S. Crowhurst, and V. Rennie (2016), Variability of neodymium isotopes associated with planktonic foraminifera in the Pacific Ocean during the Holocene and Last Glacial Maximum, *Earth Planet. Sci. Lett.*, *447*, 130–138.

Keigwin, L. D. (1998), Glacial-age hydrography of the far northwest Pacific Ocean, *Paleoceanography*, *13*, 323–339, doi:10.1029/98PA00874.

Kennett, J. P., and B. L. Ingram (1995), A 20,000 year record of ocean circulation and climate-change from the Santa-Barbara basin, *Nature*, *377*, 510–514.

Key, R. M., A. Kozyr, C. L. Sabine, K. Lee, R. Wanninkhof, J. L. Bullister, R. A. Feely, F. J. Millero, C. Mordy, and T. H. Peng (2004), A global ocean carbon climatology: Results from Global Data Analysis Project (GLODAP), *Global Biogeochem. Cycles*, *18*, GB4031, doi:10.1029/2004GB002247.

Kienast, S. S., M. Kienast, A. C. Mix, S. E. Calvert, and R. Francois (2007), Thorium-230 normalized particle flux and sediment focusing in the Panama Basin region during the last 30,000 years, *Paleoceanography*, *22*, PA2213, doi:10.1029/2006PA001357.

Kim, S. T., and J. R. O'Neil (1997), Equilibrium and nonequilibrium oxygen isotope effects in synthetic carbonates, *Geochim. Cosmochim. Acta*, *61*, 3461–3475.

Knudson, K. P., and A. C. Ravelo (2015a), North Pacific Intermediate Water circulation enhanced by the closure of the Bering Strait, *Paleoceanography*, *30*, 1–18, doi:10.1002/2015PA002840.

Knudson, K. P., and A. C. Ravelo (2015b), Enhanced subarctic Pacific stratification and nutrient utilization during glacials over the last 1.2 Myr, *Geophys. Res. Lett.*, *42*, 9870–9879, doi:10.1002/2015GL066317.

Kroopnick, P. M. (1985), The distribution of ^{13}C of ΣCO_2 in the world oceans, *Deep- Sea Res. Part A*, *32*, 57–84.

Leduc, G., L. Vidal, K. Tachikawa, F. Rostek, C. Sonzogni, L. Beaufort, and E. Bard (2007), Moisture transport across Central America as a positive feedback on abrupt climatic changes, *Nature*, *445*, 908–911.

Leduc, G., L. Vidal, K. Tachikawa, and E. Bard (2010), Changes in Eastern Pacific ocean ventilation at intermediate depth over the last 150 kyr BP, *Earth Planet. Sci. Lett.*, *298*, 217–228.

Locarnini, R. A., A. V. Mishonov, J. I. Antonov, T. P. Boyer, H. E. Garcia, O. K. Baranova, M. M. Zweng, and D. R. Johnson (2010), In *World Ocean Atlas 2009, Volume 1: Temperature*, *NOAA Atlas NESDIS*, vol. 68, edited by S. Levitus, pp. 184 , U.S. Gov. Print. Off., Washington, D. C.

Lund, D. C., and A. C. Mix (1998), Millennial-scale deep water oscillations: Reflections of the North Atlantic in the deep Pacific from 10 to 60 ka, *Paleoceanography*, *13*, 10–19, doi:10.1029/97PA02984.

Lund, D. C., A. C. Mix, and J. Southon (2011), Increased ventilation age of the deep northeast Pacific Ocean during the last deglaciation, *Nat. Geosci.*, *4*(11), 771-774.

Lynch-Stieglitz, J., R. G. Fairbanks, and C. D. Charles (1994), Glacial-interglacial history of Antarctic Intermediate Water: Relative strengths of Antarctic versus Indian Ocean sources, *Paleoceanography*, *9*, 7–29, doi:10.1029/93PA02446.

Mackensen, A., S. Schumacher, J. Radke, and D. N. Schmidt (2000), Microhabitat preferences and stable carbon isotopes of endobenthic foraminifera: Clue to quantitative reconstruction of oceanic new production?, *Mar. Micropaleontol.*, *40*, 233–258.

Marchitto, T. M., S. J. Lehman, J. D. Ortiz, J. Fluckiger, and A. van Geen (2007), Marine radiocarbon evidence for the mechanism of deglacial atmospheric CO_2 rise, *Science*, *316*, 1456–1459.

Matsumoto, K., T. Oba, J. Lynch-Stieglitz, and H. Yamamoto (2002a), Interior hydrography and circulation of the glacial Pacific Ocean, *Quat. Sci. Rev.*, *21*, 1693–1704.

Matsumoto, K., J. L. Sarmiento, and M. A. Brzezinski (2002b), Silicic acid leakage from the Southern Ocean: A possible explanation for glacial atmospheric pCO_2, *Global Biogeochem. Cycles*, *16*(3), 1031, doi:10.1029/2001GB001442.

Max, L., J. R. Riethdorf, R. Tiedemann, M. Smirnova, L. Lembke-Jene, K. Fahl, D. Nürnberg, A. Matul, and G. Mollenhauer (2012), Sea surface temperature variability and sea-ice extent in the subarctic northwest Pacific during the past 15,000 years, *Paleoceanography*, *27*, PA3213, doi:10.1029/2012PA002292.

Max, L., L. Lembke-Jene, J. R. Riethdorf, R. Tiedemann, D. Nürnberg, H. Kühn, and A. Mackensen (2014), Pulses of enhanced North Pacific Intermediate Water ventilation from the Okhotsk Sea and Bering Sea during the last deglaciation, *Clim. Past*, *10*, 591–605.

Méheust, M., R. Stein, K. Fahl, L. Max, and J. R. Riethdorf (2016), High-resolution IP_{25}-based reconstruction of sea-ice variability in the western North Pacific and Bering Sea during the past 18,000 years, *Geo-Mar. Lett.*, *36*(2), 1–11.

Mix, A. C., N. G. Pisias, R. Zahn, W. Rugh, C. Lopez, and K. Nelson (1991), Carbon 13 in Pacific deep and intermediate waters, 0–370 ka: Implications for ocean circulation and Pleistocene CO_2, *Paleoceanography*, *6*, 205–226, doi:10.1029/90PA02303.

Mook, W. G., J. C. Bommerso, and W. H. Staverma (1974), Carbon isotope fractionation between dissolved bicarbonate and gaseous carbon-dioxide, *Earth Planet. Sci. Lett.*, *22*, 169–176.

Muratli, J. M., Z. Chase, A. C. Mix, and J. McManus (2010), Increased glacial-age ventilation of the Chilean margin by Antarctic Intermediate Water, *Nat. Geosci.*, *3*(1), 23–26.

Noble, T. L., A. M. Piotrowski, and I. N. McCave (2013), Neodymium isotopic composition of intermediate and deep waters in the glacial southwest Pacific, *Earth Planet. Sci. Lett.*, *384*, 27–36.

Okazaki, Y., T. Sagawa, H. Asahi, K. Horikawa, and J. Onodera (2012), Ventilation changes in the western North Pacific since the last glacial period, *Clim. Past*, *8*, 17–24.

Ortiz, J. D., A. C. Mix, W. Rugh, J. M. Watkins, and R. W. Collier (1996), Deep-dwelling planktonic foraminifera of the northeastern Pacific Ocean reveal environmental control of oxygen and carbon isotopic disequilibria, *Geochim. Cosmochim. Acta*, *60*, 4509–4523.

Pahnke, K., and R. Zahn (2005), Southern hemisphere water mass conversion linked with North Atlantic climate variability, *Science*, *307*, 1741–1746.

Pena, L. D., I. Cacho, P. Ferretti, and M. A. Hall (2008), El Niño-Southern Oscillation-like variability during glacial terminations and interlatitudinal teleconnections, *Paleoceanography*, *23*, PA3101, doi:10.1029/2008PA001620.

Pena, L. D., S. L. Goldstein, S. R. Hemming, K. M. Jones, E. Calvo, C. Pelejero, and I. Cacho (2013), Rapid changes in meridional advection of Southern Ocean intermediate waters to the tropical Pacific during the last 30 kyr, *Earth Planet. Sci. Lett.*, *368*, 20–32.

Petit, J. R., et al. (1999), Climate and atmospheric history of the past 420,000 years from the Vostok ice core, Antarctica, *Nature*, *399*, 429–436.

Pichevin, L. E., B. C. Reynolds, R. S. Ganeshram, I. Cacho, L. Pena, K. Keefe, and R. M. Ellam (2009), Enhanced carbon pump inferred from relaxation of nutrient limitation in the glacial ocean, *Nature*, *459*, 1114–1118.

Rafter, P. A., and D. M. Sigman (2016), Spatial distribution and temporal variation of nitrate nitrogen and oxygen isotopes in the upper equatorial Pacific Ocean, *Limnol. Oceanogr.*, *61*(1), 14–31.

Rella, S. F., R. Tada, K. Nagashima, M. Ikehara, T. Itaki, K. Ohkushi, T. Sakamoto, N. Harada, and M. Uchida (2012), Abrupt changes of intermediate water properties on the northeastern slope of the Bering Sea during the last glacial and deglacial period, *Paleoceanography*, *27*, PA3203, doi:10.1029/2011PA002205.

Riethdorf, J. R., D. Nürnberg, L. Max, R. Tiedemann, S. A. Gorbarenko, and M. I. Malakhov (2013), Millennial-scale variability of marine productivity and terrigenous matter supply in the western Bering Sea over the past 180 kyr, *Clim. Past*, *9*, 1345–1373.

Rippert, N., D. Nürnberg, J. Raddatz, E. Maier, E. Hathorne, J. Bijma, and R. Tiedemann (2016), Constraining foraminiferal calcification depths in the western Pacific warm pool, *Mar. Micropaleontol.*, *128*, 14–27.

Robinson, R. S., P. Martinez, L. D. Pena, and I. Cacho (2009), Nitrogen isotopic evidence for deglacial changes in nutrient supply in the eastern equatorial Pacific, *Paleoceanography*, *24*, PA4213, doi:10.1029/2008PA001702.

Robinson, R. S., M. A. Brzezinski, C. P. Beucher, M. G. S. Horn, and P. Bedsole (2014), The changing roles of iron and vertical mixing in regulating nitrogen and silicon cycling in the Southern Ocean over the last glacial cycle, *Paleoceanography*, *29*, 1179–1195, doi:10.1002/2014PA002686.

Robinson, R. S., D. M. Sigman, P. J. DiFiore, M. M. Rohde, T. A. Mashiotta, and D. W. Lea (2005), Diatom-bound N-15/N-14: New support for enhanced nutrient consumption in the ice age subantarctic, *Paleoceanography*, *20*, PA3003, doi:10.1029/2004PA001114.

Ronge, T. A., S. Steph, R. Tiedemann, M. Prange, U. Merkel, D. Nürnberg, and G. Kuhn (2015), Pushing the boundaries: Glacial/interglacial variability of intermediate and deep waters in the southwest Pacific over the last 350,000 years, *Paleoceanography*, *30*, 23–38, doi:10.1002/2014PA002727.

Sarmiento, J. L., N. Gruber, M. A. Brzezinski, and J. P. Dunne (2004), High-latitude controls of thermocline nutrients and low latitude biological productivity, *Nature*, *427*, 56–60.

Schlitzer, R. (2015), Data analysis and visualization with ocean data view, *CMOS Bull. SCMO*, *43*(1), 9–13.

Schlung, S. A., et al. (2013), Millennial-scale climate change and intermediate water circulation in the Bering Sea from 90 ka: A high-resolution record from IODP Site U1340, *Paleoceanography*, *28*, 54–67, doi:10.1029/2012PA002365.

Schweizer, M., J. Pawlowski, T. Kouwenhoven, and B. van der Zwaan (2009), Molecular phylogeny of common cibicidids and related rotaliida (foraminifera) based on small subunit eDNA sequences, *J. Foraminiferal Res.*, *39*, 300–315.

Shackleton, N. J. (1974), Attainment of isotopic equilibrium between ocean water and the benthic foraminifera genus Uvigerina: Isotopic changes in the ocean during the last glacial, *Centre Natl de la Recherche Sci. Colloqium Int.*, *219*, 203–209.

Shcherbina, A. Y., L. D. Talley, and D. L. Rudnick (2003), Direct observations of North Pacific ventilation: Brine rejection in the Okhotsk Sea, *Science*, *302*(5652), 1952–1955.

Spero, H. J., and D. W. Lea (2002), The cause of carbon isotope minimum events on glacial terminations, *Science*, *296*(5567), 522–525, doi:10.1126/science.1069401.

Stott, L. D., M. Neumann, and D. Hammond (2000), Intermediate water ventilation on the northeastern Pacific margin during the late Pleistocene inferred from benthic foraminiferal $\delta^{13}C$, *Paleoceanography*, *15*, 161–169, doi:10.1029/1999PA000375.

Stott, L., J. Southon, A. Timmermann, and A. Koutavas (2009), Radiocarbon age anomaly at intermediate water depth in the Pacific Ocean during the last deglaciation, *Paleoceanography*, *24*, PA2223, doi:10.1029/2008PA001690.

Svensson, A., et al. (2008), A 60 000 year Greenland stratigraphic ice core chronology, *Clim. Past*, *4*, 47–57.

Takahashi, T., et al. (2002), Global sea-air CO_2 flux based on climatological surface ocean pCO_2, and seasonal biological and temperature effects, *Deep Sea Res., Part II*, *49*, 1601–1622.

Talley, L. D. (1993), Distribution and formation of North Pacific Intermediate Water, *J. Phys. Oceanogr.*, *23*(3), 517–537.

Tanaka, S., and K. Takahashi (2005), Late Quaternary paleoceanographic changes in the Bering Sea and the western subarctic Pacific based on radiolarian assemblages, *Deep Sea Res., Part II*, *52*(16–18), 2131–2149.

Wejnert, K. E., R. C. Thunell, and Y. Astor (2013), Comparison of species-specific oxygen isotope paleotemperature equations: Sensitivity analysis using planktonic foraminifera from the Cariaco Basin, Venezuela, *Mar. Micropaleontol.*, *101*, 76–88.